Precision Engineering 33 (2009) 175–186

Contents lists available at ScienceDirect

Precision Engineering

journal homepage: www.elsevier.com/locate/precision

A practical control method for precision motion—Improvement of NCTF control method for continuous motion control

Kaiji Sato*, Guilherme Jorge Maeda

Interdisciplinary Graduate School of Science and Engineering, Tokyo Institute of Technology, 4259 Nagatsuta, Midori-ku, Yokohama 226-8502, Japan

ARTICLE INFO

Article history:
Received 16 January 2008
Received in revised form 2 May 2008
Accepted 10 May 2008
Available online 10 July 2008

Keywords:
Precision
Motion control
Tracking control
Contouring control
Positioning
Continuous motion
Ball screw
NCTF control

ABSTRACT

The present paper describes a practical control method for a precision motion system and the performance thereof. For practical use, high motion control performance and ease of design and controller adjustment are desired. A nominal characteristic trajectory following control (NCTF control) has been investigated to realize high performance and ease of application of point-to-point (PTP) positioning. The controller comprising a nominal characteristic trajectory (NCT) and a PI compensator is free from exact modeling and parameter identification. In the present paper, the NCTF control is modified in order to improve the control performance of continuous motions such as tracking and contouring motions. The NCTF controller for continuous motion (referred to as Continuous Motion NCTF controller) has a structure that is almost identical to the conventional NCTF controller and is designed using the same design procedure. The Continuous Motion NCTF controller is applied to ball screw mechanisms, and its motion control performance is evaluated from the experimental tracking, contouring, and positioning control results. The experimental results prove that the Continuous Motion NCTF controller achieves the same positioning performance as the conventional NCTF controller, and generally achieves better continuous motion control performances than PI-D or conventional NCTF controllers. In 0.25 Hz and 100-nm radius circular motion, the experimental tracking errors for Continuous Motion NCTF were smaller than 10 nm.

1. Introduction

Precision motion systems are important components of industrial machines such as machine tools, measuring machines, wire bonders, and semiconductor manufacturing systems. The motion accuracy and response of these systems have a decisive influence on the machine performances. Tracking, contouring, and positioning motions are important for motion control systems and are often used to evaluate the performance of such systems. These motions are also required in industrial machines. General-purpose servo controllers are desired in order to realize high performance for all motions, and machining centers require high performance for all motions.

Several advanced control methods have been proposed, and these control methods have been applied to precision motion mechanisms for performance evaluation. However, classical controllers that include PID and/or lead-lag elements are still the most widely used type of controller [1,2]. Several non-contact ultra-precision motion systems, such as steppers and ultra-precision machine tools, also have classical controllers [3,4]. This indicates that simplicity based on simple structures, high adoptability, and ease of understanding, design, and control parameter adjustment are significant in industrial application. Controllers based on classical control theory have the advantage of this simplicity. However, several precision motion mechanisms have nonlinear characteristics, as represented by friction, and their mechanism characteristics sometimes vary. Thus, high robust characteristics are also required in practical application.

Although conventional classical controllers are convenient, their robust characteristics are often insufficient for precision motion. For the solution of this problem, the use of several model-based controllers is increasing. Friction compensators are classical elements for the solution of the friction problem [5–7]. In addition, disturbance observers with nominal object models [8–10] and friction models [11–14] have often been used to eliminate the influence of nonlinear characteristics, including those of friction and characteristic variation. Friction compensators and disturbance observers are generally used with PID controllers. Recently, a number of studies have examined sliding mode controllers for highly robust precision positioning [11,15–17]. However, exact modeling of mechanisms, their accurate parameter identification, and sufficient knowledge of their controllers are needed in their design procedures. This has led to controller designers avoiding the use of sliding mode controllers.

* Corresponding author. Tel.: +81 45 924 5045; fax: +81 45 924 5483.
E-mail address: kaiji@pms.titech.ac.jp (K. Sato).

0141-6359/$ – see front matter © 2008 Elsevier Inc. All rights reserved.
doi:10.1016/j.precisioneng.2008.05.006

In order to improve the reference following performance of conventional control systems, additional elements have been investigated [18]. Feedforward filter elements have been proposed for the improvement of tracking performance, and the advantages of these elements have been shown [19–21]. However, these require exact model and accurate model parameters. Their effects are sensitive to model errors. For high contouring motion performance, cross-coupled controllers (CCC) have been investigated [22–24]. In some applications, the effectiveness of the CCC has been reported. However, its design also requires exact model and accurate model parameters. Thus, the use of these additional elements leads to complex controller structures and time-consuming designs. Moreover, in general, only designers with considerable knowledge of mechanisms and control theory are able to implement such controllers. Consequently, classical controllers are still widely used in industrial applications due to their simple structure and easy design.

A nominal characteristic trajectory following (NCTF) control method has been investigated as the method overcoming these problems for point-to-point (PTP) positioning [25–29]. The controller comprises a nominal characteristic trajectory (NCT) and a PI compensator. The controller may look like model-based controllers, such as the siding mode controller or the seeking mode controller of HDD [31,32]. However, in contrast to the model-based controllers, the NCTF controller does not require exact modeling or model parameter identification and is easy to design. NCTF control systems provide better positioning results than conventional PID control systems. The purpose of the present study is to improve the NCTF control method for continuous motion applications such as tracking and contouring motions. The NCTF controller for continuous motion (referred to as the Continuous Motion NCTF controller) has almost the same structure as the conventional controller and is designed using the same design procedure. The Continuous Motion NCTF controller is applied to ball screw mechanisms, and its motion control performance is evaluated from the experimental tracking, contouring, and positioning control results.

In Section 2, the experimental setup is introduced and the characteristics of the mechanism are described. Section 3 explains the improvement of the NCTF controller for continuous motion (the Continuous Motion NCTF controller) and the concrete design procedure. In Section 4, motion control performances of the Continuous Motion NCTF control system, such as tracking, contouring, and positioning control performances, are evaluated and compared with those of conventional NCTF and PI-D control systems with ball screw mechanisms. Finally, Section 5 presents the conclusions of the present study.

2. Experimental setup

The ball screw mechanisms used herein are shown in Fig. 1. These mechanisms have similar structures, but their movable mass conditions differ. The mechanism with the large additional mass is referred to as the *X*-axis mechanism, and the other is referred to as the *Y*-axis mechanism. The mechanisms are driven as if the two-axis mechanisms were conceptually stacked as in an *XY* table configuration. The *Y*-axis mechanism is the ball screw mechanism used in ref. [29]. Its dynamic model is represented by Fig. 2. The additional mass fixed on the table of the *X*-axis mechanism is similar to the total mass of the *Y*-axis mechanism. Table 1 shows the model parameters. In addition to the table mass, the spring constant K_n and the damping coefficient C_n of the *X*-axis mechanism are larger than those of the *Y*-axis mechanism. For the *X*-axis mechanism, the compliance becomes significant compared to the heavy mass on the table, which leads to vibration, but not for the *Y*-axis mechanism. The controller sampling frequency is 5 kHz, and the feedback position is determined by a laser position sensor with a resolution of 1.24 nm (Agilent: 10897B). The lead of the ball screw is 2 mm/rev, and the maximum travel of the table is 55 mm.

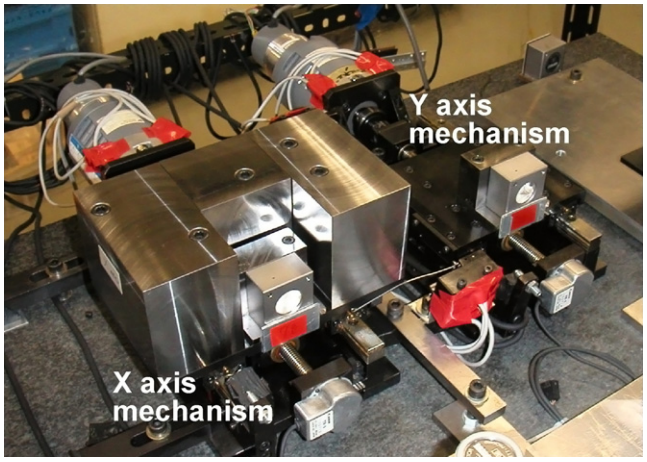

Fig. 1. Two-axis ball screw mechanism.

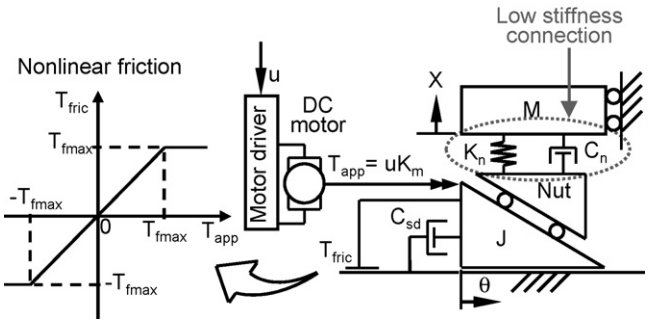

Fig. 2. Dynamic model of a ball screw mechanism.

3. Improvement of NCTF controller for continuous motion control

3.1. Structure

3.1.1. Conventional NCTF control system

Fig. 3 shows the structure of a conventional NCTF control system designed for PTP positioning. Its controller is composed of a nominal characteristic trajectory element and a PI compensator. The objective of the PI compensator is to make the mechanism motion follow the NCT, finishing at the origin of the NCT. The output of the NCT element is a signal, u_p, which is the difference between the

Table 1
Model parameters.

Symbol	Description (unit)	Mechanism	
		X-axis	*Y*-axis
M	Table mass (kg)	17.50	3.57
J	Moment of inertia (kg m^2)	1.81×10^{-4}	
K_m	Torque constant of the motor (Nm/A)	0.172	
T_{fmax}	Coulomb friction (Nm)	0.090	0.046
C_{sd}	Viscous friction (Nms/rad)	0.00100	0.00097
K_n	Spring constant (N/m)	4.5×10^7	8.3×10^5
C_n	Damping coefficient (Ns/m)	2300	1700
T_{fric}	Nonlinear friction (Nm)	–	–
T_{app}	Torque applied to the ball screw (Nm)	–	–

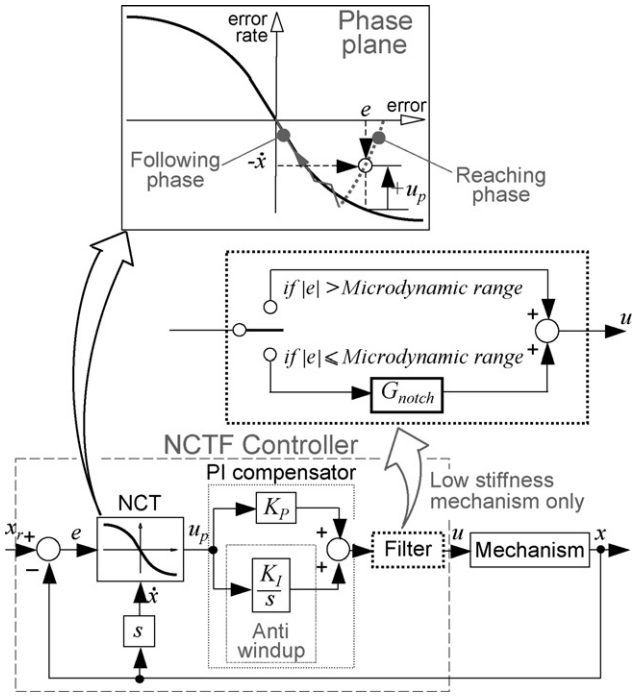

Fig. 3. Structure of the conventional NCTF control system.

actual error rate of the mechanism ($-\dot{x}$) and the error rate of the NCT. On the phase-plane, the mechanism motion is divided into a reaching phase and a following phase. During the reaching phase, the PI compensator controls the mechanism motion to reach the NCT as quickly as possible. During the following phase, the PI compensator controls the mechanism motion to follow the NCT, leading the motion to the origin of the phase-plane. In order to reduce the overshoot caused by integrator windup, a conditional freeze integrator is used. The rule is as follows:

$$\Delta u_{\mathrm{i}} = \begin{cases} 0, & |u_{\mathrm{o}} + u_{\mathrm{i}}| > u_{\mathrm{s}} \quad \text{and} \quad e u_{\mathrm{i}} \geq 0 \\ e, & \text{otherwise} \end{cases} \tag{1}$$

where u_{o} is the proportional control signal, u_{i} is the integral control signal, Δu_{i} is the change rate of u_{i}, and u_{s} is the maximum value of the control signal. The filter in Fig. 3 is a conditional notch filter for reducing residual vibration and becomes active only in a microdynamic range.

The NCT is constructed using the velocity of a mechanism having damping characteristics because the motion of the mechanism is essentially influenced by the velocity. The NCT is used for determining the virtual velocity reference for each deviation and the PI

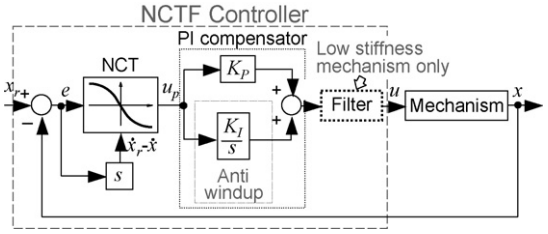

Fig. 4. Structure of the Continuous Motion NCTF control system (I).

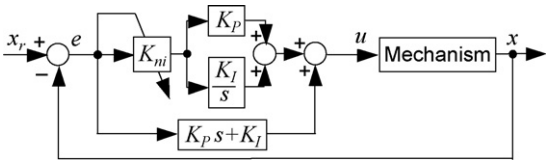

Fig. 5. Structure of the Continuous Motion NCTF control system (II).

compensator works for velocity control in the conventional NCTF controller (see Fig. 3). In PTP positioning, the reference rate ($\dot{x}_{\mathrm{r}}$) is not important. The NCT without the information of the reference rate is suitable for PTP positioning and can be followed by the actual mechanism. However, this structure tends to produce low reference following characteristics at high reference rates.

3.1.2. Improvement for continuous motion

Fig. 4 shows the Continuous Motion NCTF controller structure improved for continuous motion. Based on the conventional NCTF controller, the Continuous Motion NCTF controller is obtained by considering the value of $\dot{x}_{\mathrm{r}}$. The input signal to the PI compensator includes the reference rate ($\dot{x}_{\mathrm{r}}$). The reference rate ($\dot{x}_{\mathrm{r}}$) helps the mechanism to move rapidly. When the error and the reference rate are large, the mechanism with the Continuous Motion NCTF controller may not sufficiently follow the NCT. However, in continuous motion, controllers usually act near the reference, and the action far from the reference is not important.

Notice that the complexity of the controller does not increase. At the same time, when $\dot{x}_{\mathrm{r}}$ is zero, the structure in Fig. 4 is identical to the structure in Fig. 3. Therefore, the Continuous Motion NCTF controller has the same control law as the conventional NCTF controller during PTP positioning.

The Continuous Motion NCTF control system can be represented by Fig. 5. When the simplified dynamic model of the mechanism is expressed as Eq. (1), the transfer function of the Continuous Motion NCTF control system $G_{\mathrm{CM}}(s)$ is expressed as Eq. (2).

$$\frac{X}{U} = K\frac{\alpha}{s(s+\alpha)} \tag{1}$$

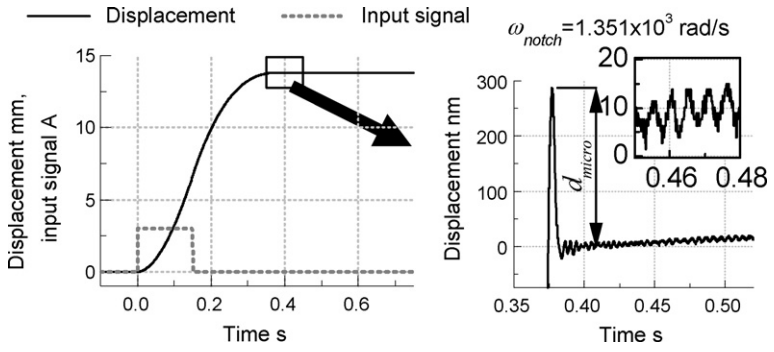

Fig. 6. Open-loop step response of the *X*-axis mechanism.

$$G_{CM}(s) = \frac{X}{X_r} = \frac{2\zeta\omega_n s + \omega_n^2}{\left(\frac{s+\alpha}{s+K_{nl}}\right)s^2 + 2\zeta\omega_n s + \omega_n^2} \quad (2)$$

where the PI compensator gains are expressed as Eq. (3).

$$K_P = \frac{2\zeta\omega_n}{\alpha K} \quad (3a)$$

$$K_I = \frac{\omega_n^2}{\alpha K} \quad (3b)$$

The transfer function of the conventional NCTF control system $G_{PTP}(s)$ is given as Eq. (4) [29].

$$G_{PTP}(s) = \frac{K_{nl}}{s+K_{nl}} \times G_{CM}(s) = G_{1st}(s) \times G_{CM}(s) \quad (4)$$

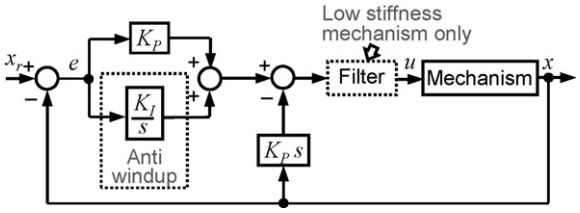

Fig. 7. PI-D control system for comparison.

In the NCTF controller design, $G_{CM}(s)$ is adjusted so as to have the higher bandwidth than $G_{1st}(s)$. Therefore, the Continuous Motion NCTF control system has higher bandwidth than the conventional NCTF control system. However, when

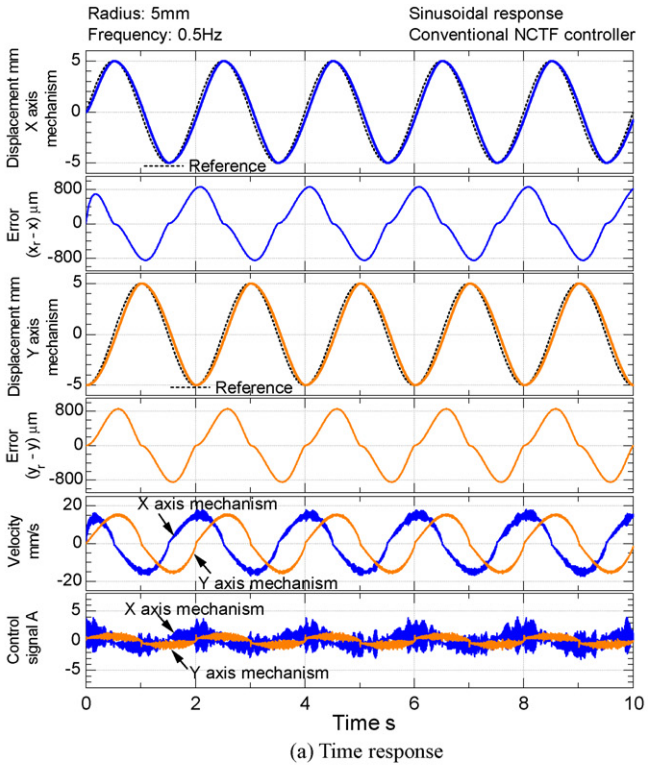

(a) Time response

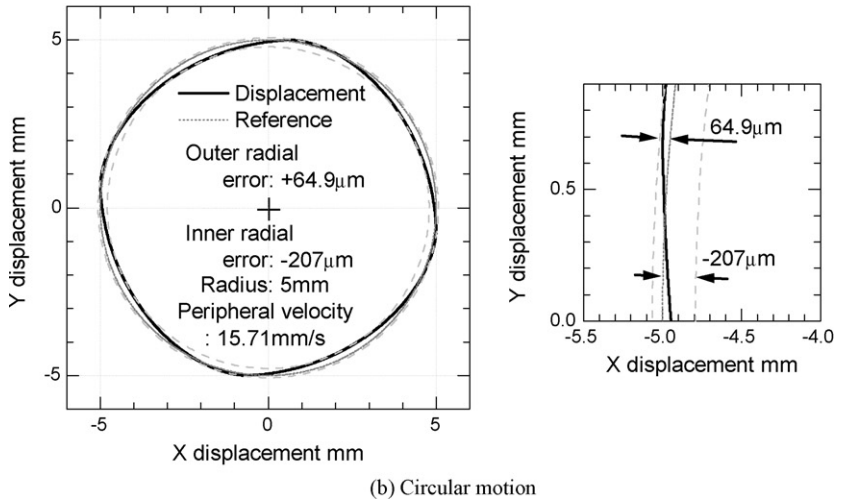

(b) Circular motion

Fig. 8. Continuous motion performances with the conventional NCTF controller.

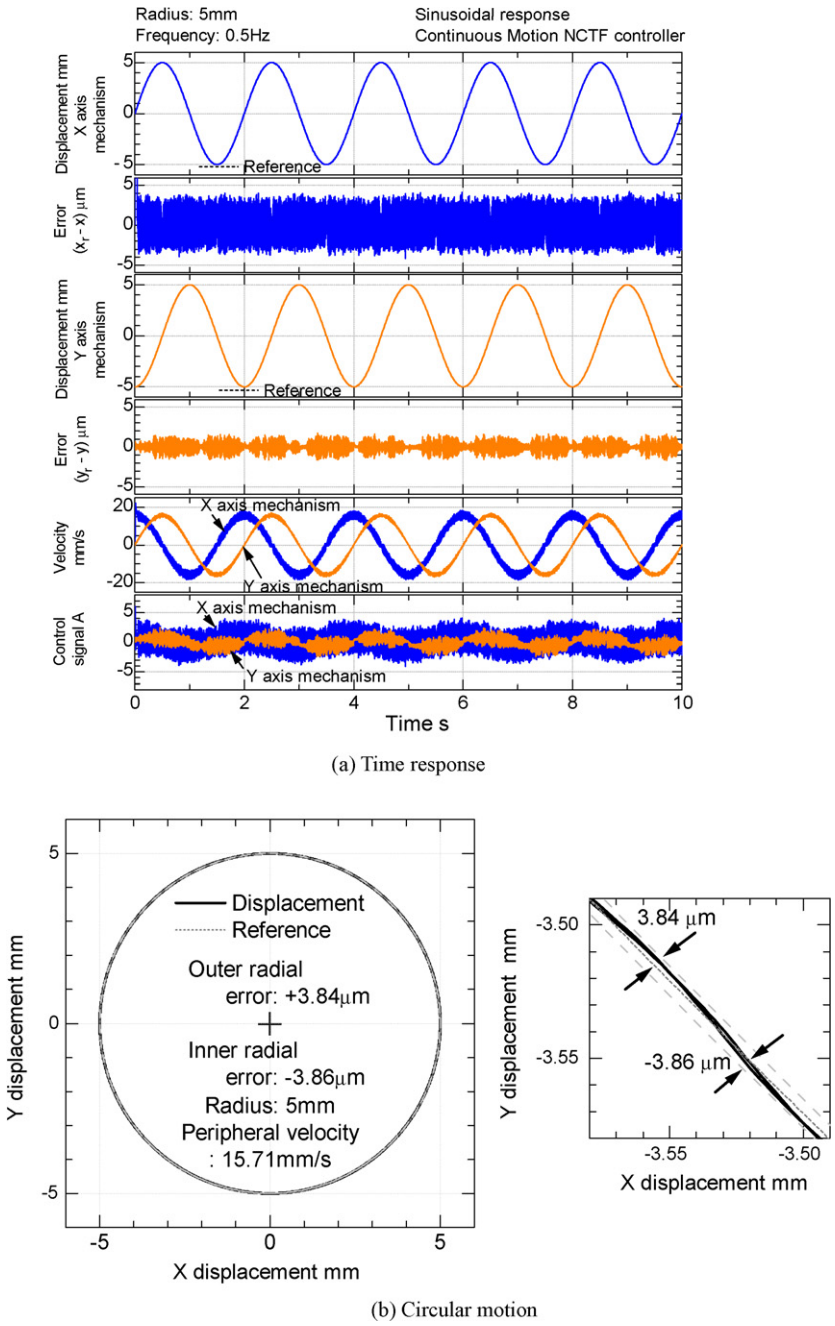

(a) Time response

(b) Circular motion

Fig. 9. Continuous motion performances with the Continuous Motion NCTF controller.

a step reference signal is applied to the Continuous Motion NCTF control system, its initial controller output includes an impulse signal which tends to produce an unexpected vibration in the table motion. Thus the influence of the impulse signal on PTP positioning performance is examined in Section 4.2.

3.2. Design procedure

As mentioned in Subsection 3.1, the Continuous Motion NCTF controller has almost the same controller structure as the conventional controller. As a result, the design procedure of the conventional NCTF controller is used for the Continuous Motion

Table 2
Motion control performances of the conventional and the Continuous Motion NCTF controllers.

Controller	max $\lvert x_r - x \rvert$		max $\lvert y_r - y \rvert$		Maximum radial error	
	Average (μm)	Standard deviation (μm)	Average (μm)	Standard deviation (μm)	Average (μm)	Standard deviation (μm)
Conventional NCTF	8.55×10^2	3.08×10^{-1}	8.53×10^2	8.45×10^{-2}	2.06×10^2	1.414×10^{-1}
Continuous Motion NCTF	4.47	2.30×10^{-1}	1.626	1.076×10^{-1}	3.891	1.914×10^{-1}

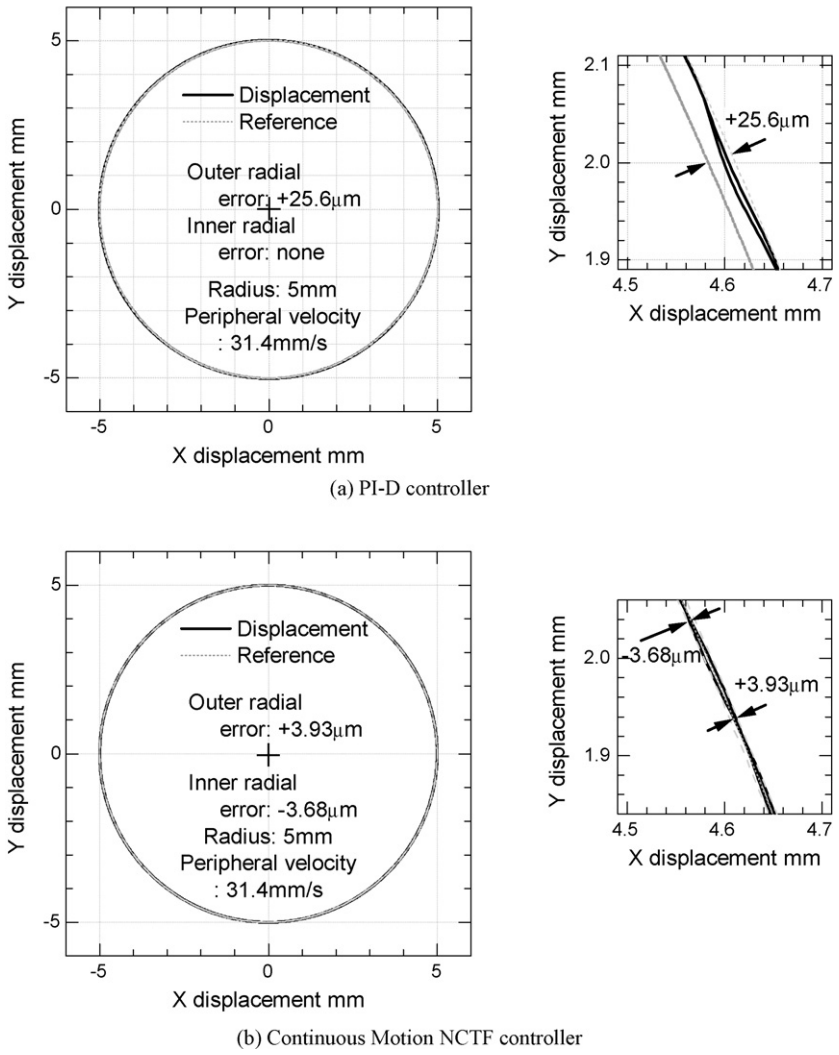

Fig. 10. Circular motion with reference input A in Table 3 (peripheral velocity: 31.4 mm/s).

NCTF controller without modification. The NCTF control system is basically designed according to the following procedure [29].

(I) *NCT construction*: From the open-loop response of the mechanism, the NCT is constructed on the phase-plane. The NCT is linearized close to the origin of the phase-plane, with inclination m. m is equal to $-\alpha$ and K is determined from Eq. (1) and the open-loop response.

(II) *Determination of the practical stability condition*: The mechanism is driven with the NCTF controller using only the proportional element. The value of the proportional gain is increased in order to determine the ultimate proportional gain (K_{Pu}). Using K_{Pu}, the practical stability condition is given as Eq. (5).

$$\zeta < K_{Pu}\left(\frac{K\alpha}{2\omega_n}\right) \tag{5}$$

(III) *Adjustment of the PI compensator gains*: The PI compensator gains expressed as Eq. (3) are determined using the practical stability condition given as Eq. (5).

(IV) *Conditional notch filter design*: When a mechanism has a measurable vibration characteristic resulting from the low stiffness of power transmission, the conditional notch filter is designed and implemented. The conditional notch filter is active only when the magnitude of the error is equal to or less than the microdynamic range. The active range of the filter is limited so that the filter does not deteriorate the response of the control system in the macrodynamic range. The transfer function of the notch filter is expressed as:

$$G_{notch} = \frac{s^2 + \omega_{notch}^2}{s^2 + 2\zeta_{notch}\omega_{notch}s + \omega_{notch}^2} \tag{6}$$

The active range of the filter and the parameter ω_{notch} are determined from the open-loop step response. Fig. 6 shows the

Table 3
Reference input (1).

Reference input	Wave form	Amplitude (μm)	Frequency (Hz)
A	Sinusoidal	5.00×10^3	1.0
B	Sinusoidal	1.00	0.5

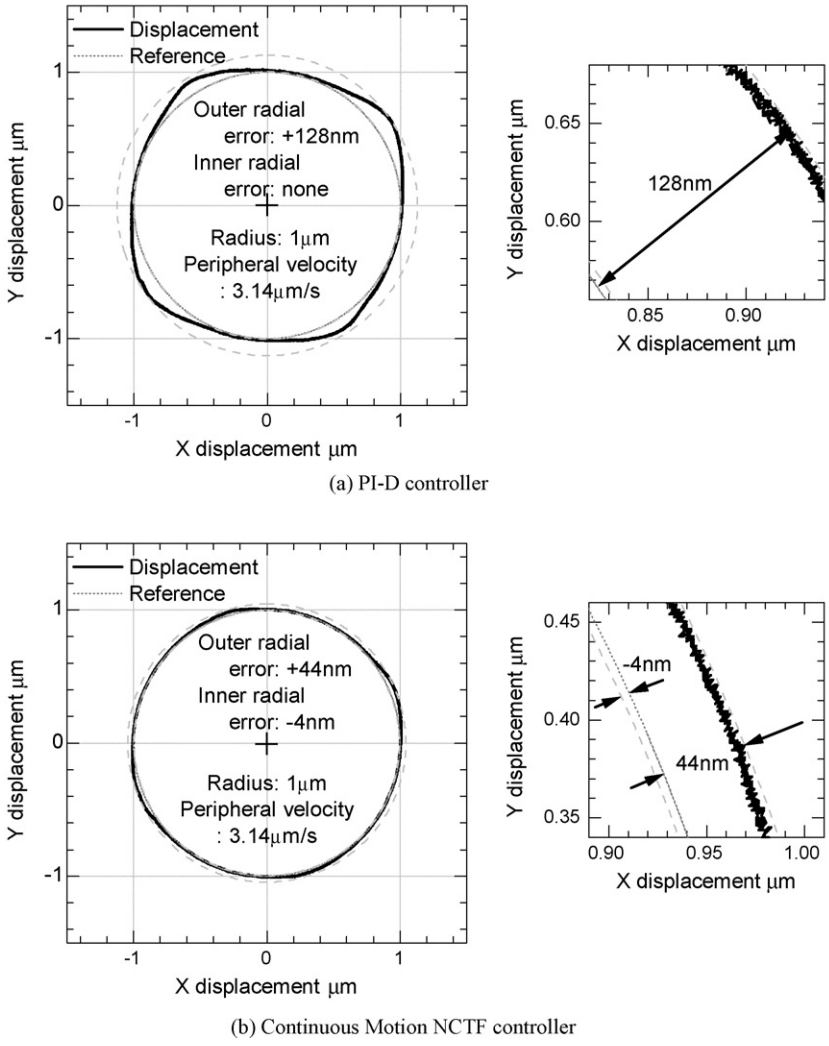

Fig. 11. Circular motion with reference input B in Table 3 (peripheral velocity: 3.14 μm/s).

Table 4
Contouring performances with the PI-D and the Continuous Motion NCTF controllers (1).

Reference input	Controller	Maximum radial error	
		Average (μm)	Standard deviation (μm)
A	PI-D	2.51×10^{1}	1.747×10^{-1}
	Continuous Motion NCTF	3.81	2.93×10^{-1}
B	PI-D	1.267×10^{-1}	1.6×10^{-3}
	Continuous Motion NCTF	4.36×10^{-2}	3.9×10^{-3}

open-loop step response of the *X*-axis mechanism. In the figure, d_{micro} represents the microdynamic range and is used as the active range of the filter. The angular frequency of the vibration was taken to be ω_{notch}. The frequency tends to change [30]. However, sufficient large ζ_{notch} can hide the influence of the change on positioning accuracy. You should determine the large ζ_{notch} which does not have a bad effect on the step response in the microdynamic range.

It should be noted that this procedure can be completed without any previous information about the model parameters. In the next section, two ball screw mechanisms are used for evaluation of the Continuous Motion NCTF control performance. Although their table

Table 5
Tracking performances with the PI-D and the Continuous Motion NCTF controllers (1).

Reference input	Controller	max $\lvert x_r - x \rvert$		max $\lvert y_r - y \rvert$	
		Average (μm)	Standard deviation (μm)	Average (μm)	Standard deviation (μm)
A	PI-D	2.51×10^{1}	1.746×10^{-1}	1.995×10^{1}	2.90×10^{-2}
	Continuous Motion NCTF	4.24	2.84×10^{-1}	1.765	9.22×10^{-2}
B	PI-D	1.781×10^{-1}	1.9×10^{-3}	1.209×10^{-1}	9.6×10^{-3}
	Continuous Motion NCTF	4.85×10^{-2}	4.1×10^{-3}	3.44×10^{-2}	5.3×10^{-3}

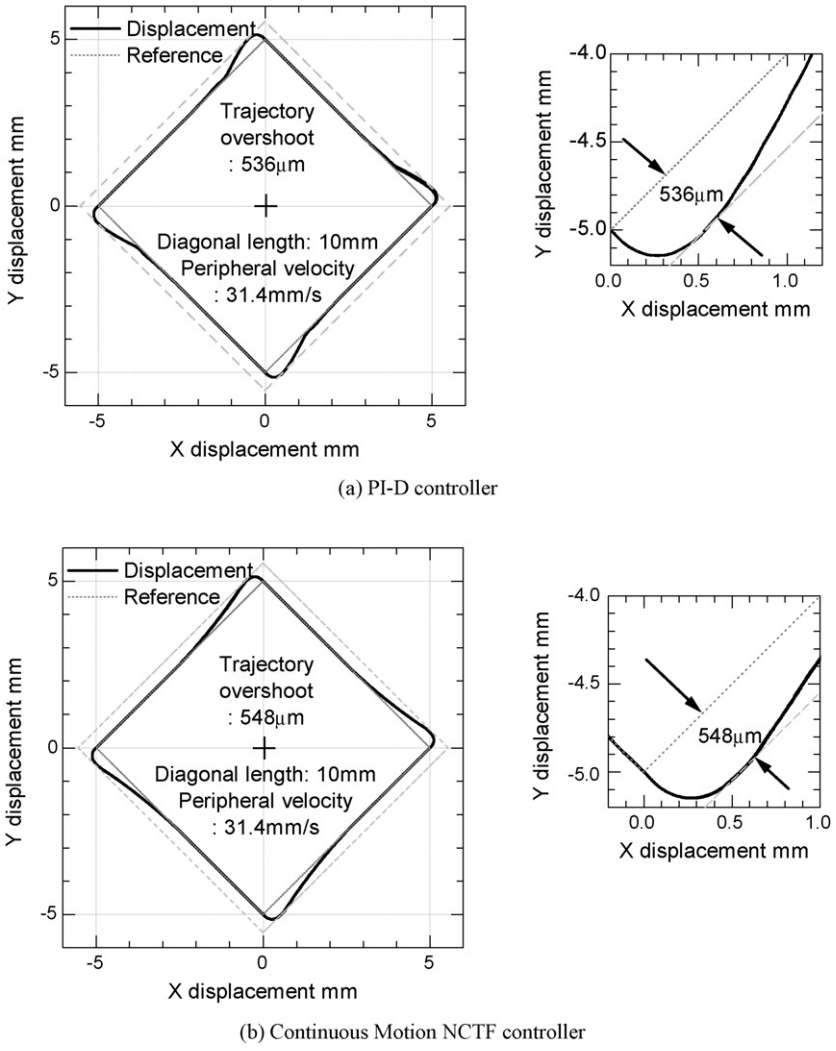

Fig. 12. Square motion with reference input C in Table 6 (peripheral velocity: 31.4 mm/s).

masses differ, the same controller parameters and the same NCT are implemented on the mechanisms for examining the robustness to the change in table mass. The conditional notch filter is not used for the *Y*-axis mechanism because the mechanism has sufficient mechanical stiffness. This procedure is applicable to any positioning mechanism composed of a damped mass and driven by an AC or DC motor.

4. Performance evaluation

In this section, three types of motion control performances, that is, tracking, contouring, and positioning performances, are experimentally examined and the effectiveness of the Continuous Motion NCTF controller is evaluated in comparison with a conventional NCTF controller and a PI-D controller. The conventional NCTF controller has the same controller parameters as the Continuous Motion NCTF controller designed through the procedure shown in Section 3.2. The NCT and controller parameters designed in ref. [29] are used. For the *X*-axis mechanism, d_{micro} and ω_{notch} were determined from Fig. 6, as the parameters of the conditional notch filter. In this paper, ζ_{notch} was set at 3. The conditional notch filter for the *X*-axis mechanism is active in all the performance evaluation when the magnitude of the error is equal to or less than the microdynamic range.

The PI-D controller has an anti-windup integrator and its controller structure is given in Fig. 7. The gains were then fine-tuned, so that the PI-D controller achieved a performance that was comparable to that of the Continuous Motion NCTF controller under a reference input of a triangular wave, the period and amplitude of which were 0.9 s and 5 mm, respectively. For the fine-tuning, the *X*-axis mechanism was used in the experiments. The tuned PI-D controller gains are $K_{\text{P}} = 297$ A/mm, $K_{\text{I}} = 1.583 \times 10^4$ A/mms, and $K_{\text{D}} = 1.47$ As/mm.

In each of the controllers, the same controller parameters are used with the *X*-axis mechanism (heavyweight condition) and *Y*-axis mechanism (lightweight condition). For the performance evaluation of continuous motion, the *X*- and *Y*-axis mechanisms are driven as a stacked type *XY* mechanism. For circular motions, sinusoidal reference inputs are applied to the mechanisms and

Table 6
Reference input (2).

Reference input	Wave form	Amplitude (μm)	Period (s)
C	Triangular	5.00×10^3	0.9
D	Triangular	1.00	1.801

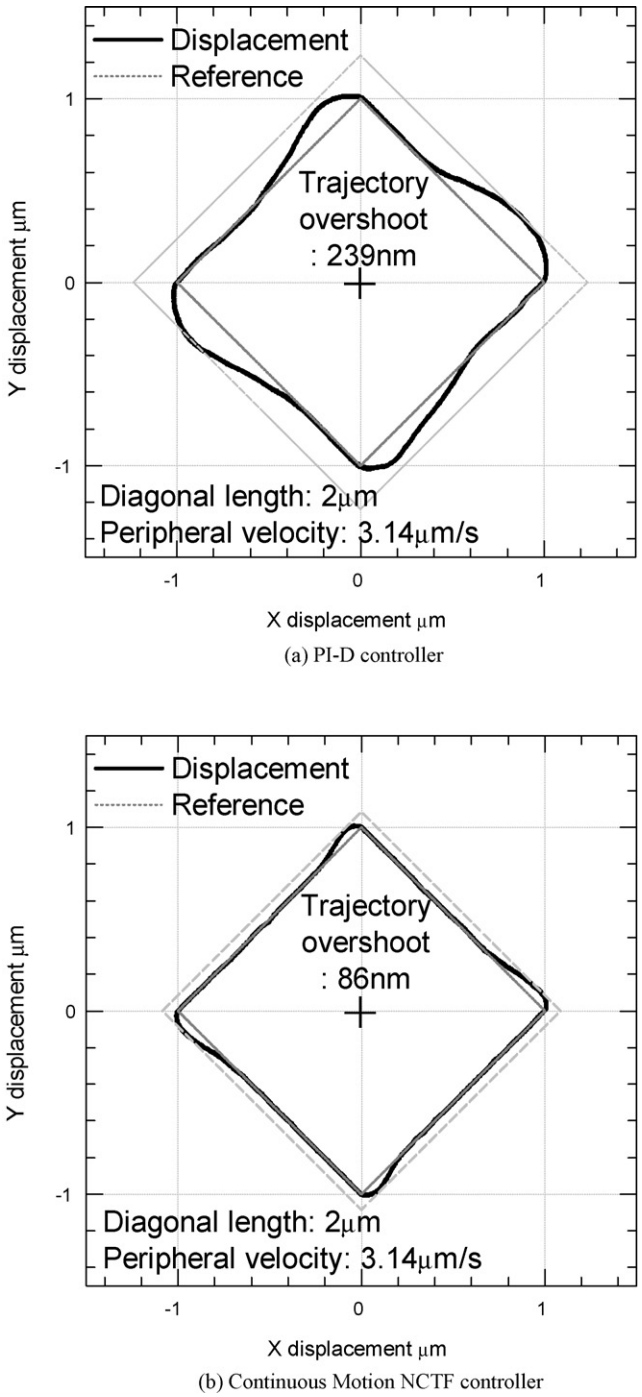

Fig. 13. Square motion with reference input D in Table 6 (peripheral velocity: 3.14 μm/s).

triangular reference inputs are used for square motions. Each experiment is repeated 20 times, and the average error and standard deviation are calculated.

4.1. Tracking and contouring control performances

4.1.1. Comparison of Continuous Motion NCTF controller with conventional NCTF controller

Fig. 8 shows the experimental continuous motion performances of the conventional controller. The performance of the Continuous Motion NCTF controller is shown in Fig. 9. The experiments are realized as if the two-axis mechanisms were conceptually stacked as in an *XY* table configuration. Thus, using a sine wave reference with the *X*-axis mechanism, and a cosine wave reference with the *Y*-axis mechanism, the resulting contour is a circle. In Fig. 9, the difference between the mechanism characteristics influences the residual vibration amplitude of tracking error but not the outline of tracking motion. The Continuous Motion NCTF controller produces smaller tracking errors than the conventional controller.

Each experiment was repeated 20 times, and the average error and standard deviation were calculated. The reference used in the experiments is a circle having a radius of 5 mm and a peripheral velocity of 15.71 mm/s (frequency of 0.5 Hz). The average errors and standard deviations of 20 similar experiments are shown in Table 2. The differences in performance between the two controllers are very large. The radial error with the Continuous Motion NCTF controller is reduced by more than 50 times, proving the suitability of the proposed controller structure for continuous motion.

Table 7
Contouring performances with the PI-D and the Continuous Motion NCTF controllers (2).

Reference input	Controller	Trajectory overshoot	
		Average (μm)	Standard deviation (μm)
C	PI-D	5.40×10^{2}	7.55
	Continuous Motion NCTF	5.49×10^{2}	5.65
D	PI-D	2.38×10^{-1}	4.4×10^{-3}
	Continuous Motion NCTF	8.77×10^{-2}	3.5×10^{-3}

4.1.2. Comparison of Continuous Motion NCTF controller with PI-D controller

Fig. 10 shows the contouring performance comparison between the PI-D and the Continuous Motion NCTF controllers with the circular reference. The contouring circular motions are calculated from the tracking motion of the *X*- and *Y*-axis mechanisms with reference input A shown in Table 3. The contouring circular motions with reference input B in Table 3 are shown in Fig. 11. The experimental maximum radial errors are summarized in Table 4. In this table, the averaged radial errors obtained using the PI-D controller are more than twice those obtained using the Continuous Motion NCTF controller. The PI-D response in Fig. 11 shows that the maximum deviation occurs at protuberances near 30°, 120°, 210°, and 300°. The same tendency is observed for the Continuous Motion NCTF controller, although the errors for the Continuous Motion NCTF controller are much smaller than those for the PI-D controller. This is attributed to the nonlinear friction of the mechanism [33].

The averaged tracking errors of 20 experiments to each reference input are summarized in Table 5. The averages of the maximum tracking errors with the PI-D controller are more than 3 times greater than that obtained using the Continuous Motion NCTF controller. Table 5 indicates the superior performance of the Continuous Motion NCTF controller.

Fig. 12 shows the contouring performance comparison between the controllers for the square reference. The contouring square motions are calculated from the tracking motion of the *X*- and *Y*-axis mechanisms with reference input C shown in Table 6. As mentioned in the beginning of this section, the tracking motion of the *X*-axis mechanism with reference input C was evaluated for tuning PI-D control parameters. The contouring square motions with reference input D in Table 6 are shown in Fig. 13. The experimental maximum trajectory overshoots are summarized in Table 7. The trajectory overshoot obtained with the PI-D controller to the reference input C is 1.6% smaller than that obtained with the Continuous Motion NCTF controller (Fig. 12). However, the use of reference input D makes the trajectory overshoot for the PI-D controller approximately 3

Table 8
Tracking performances with the PI-D and the Continuous Motion NCTF controllers (2).

Reference input	Controller	max $\lvert x_r - x \rvert$		max $\lvert y_r - y \rvert$	
		Average (μm)	Standard deviation (μm)	Average (μm)	Standard deviation (μm)
C	PI-D	5.30×10^{2}	1.537×10^{1}	5.39×10^{2}	3.51
	Continuous Motion NCTF	5.31×10^{2}	2.08×10^{1}	5.49×10^{2}	9.41
D	PI-D	2.66×10^{-1}	3.2×10^{-3}	2.05×10^{-1}	3.9×10^{-3}
	Continuous Motion NCTF	8.87×10^{-2}	3.6×10^{-3}	7.95×10^{-2}	3.9×10^{-3}

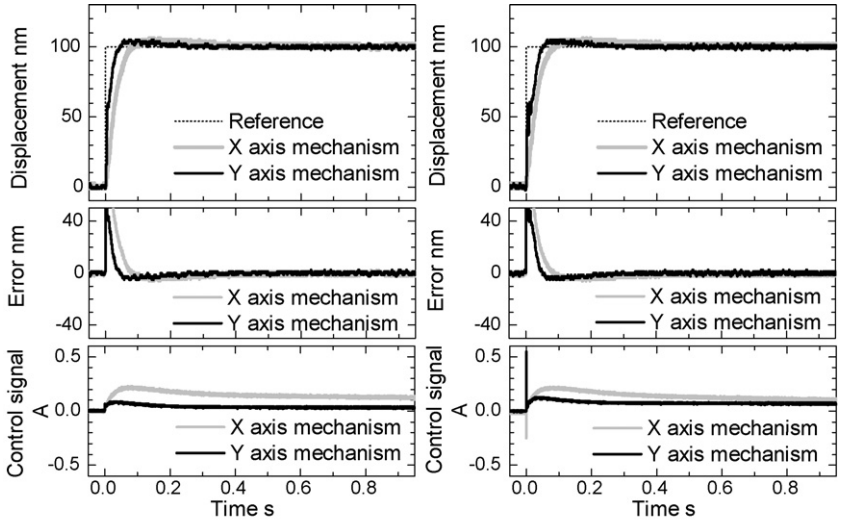

Fig. 14. PTP positioning performance comparison between the two NCTF controllers.

times larger than the Continuous Motion NCTF controller (Fig. 13). Therefore, from an overall viewpoint, the Continuous Motion NCTF controller shows better motion control performance than the PI-D controller.

The average tracking errors of 20 experiments for reference inputs in Table 6 are summarized in Table 8. The maximum tracking errors for reference input C show that the PI-D has a slightly better performance than the Continuous Motion NCTF controller. The errors of the *X*-axis mechanism motion have a negligible difference, but for the *Y*-axis mechanism, the PI-D control system has 1.8% less error. One possible reason for this is the presence of the derivative element of the PI-D controller, which has the effect of damping the mechanism motion and thus decreasing overshoot. The averaged tracking errors of the Continuous Motion NCTF controller are approximately 2.5 times smaller than those of the PI-D controller.

4.2. Positioning performance

Fig. 14 shows the responses of the conventional NCTF controller and the Continuous Motion NCTF controller to a 100-nm step input. In both controllers, the NCT and controller parameters designed in ref. [29] are used. For the *X*-axis mechanism, d_{micro} and ω_{notch} were determined from Fig. 5, as the parameters of the conditional notch filter. In this paper, ζ_{notch} was set at 3.

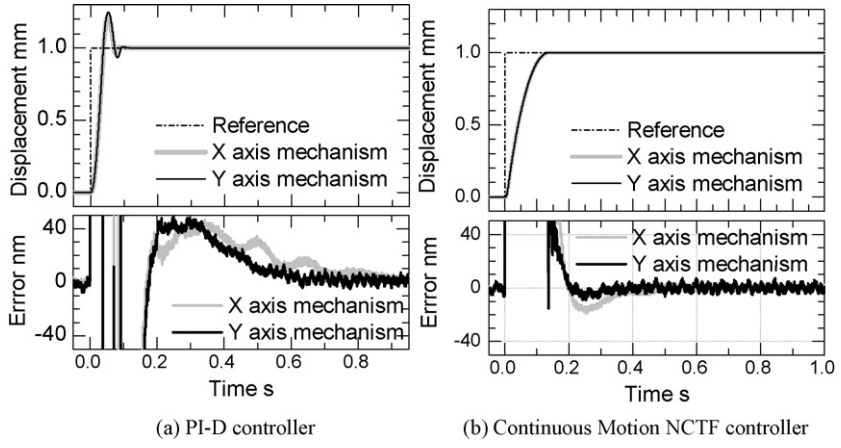

Fig. 15. PTP positioning performance comparison between the PI-D and the Continuous Motion NCTF controllers.

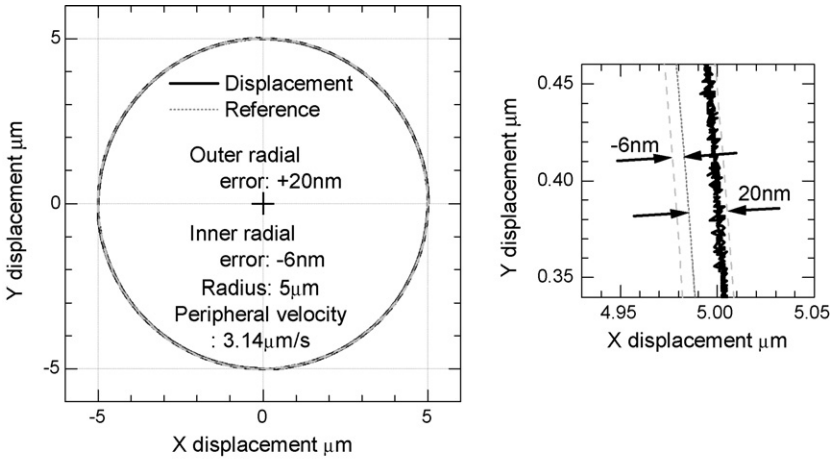

Fig. 16. Circular motion (radius: 5 μm, peripheral velocity: 3.14 μm/s, motion frequency: 0.1 Hz).

As shown in Fig. 14, the Continuous Motion NCTF controller applies impulse current to the mechanism immediately after applying a step reference input, but this is not the case for the conventional NCTF controller. However, the response for the Continuous Motion NCTF controller is similar to that for the conventional controller. The impulse current did not deteriorate the positioning performance. The positioning characteristic of the *X*-axis mechanism with the NCTF controllers is similar to that of the *Y*-axis mechanism. The result demonstrates the high robustness of the NCTF controllers to table mass change.

Fig. 15 shows the responses of the PI-D controller and the Continuous Motion NCTF controller to a 1-mm step input. The response of the *X*-axis mechanism obtained with each controller agrees well with that of the *Y*-axis mechanism. In contrast to the PI-D controller, the Continuous Motion NCTF controller causes no overshoot response for either of the mechanisms. This shows that the Continuous Motion NCTF controller has better positioning performance than the PI-D controller.

4.3. Characteristic of the Continuous Motion NCTF control system

The Continuous Motion NCTF controller can realize higher precision continuous motion than those shown in Section 4.1. Fig. 16 shows the experimental circular motion of the Continuous Motion NCTF control system using the *X*- and *Y*-axis mechanisms. The reference motion frequency is 0.1 Hz. The radius of the circular motion is 5 μm. The maximum radial error of the circular motion is 20 nm. The accuracy of the circular motion is influenced by the motion frequency. Low reference motion frequency tends to make the motion accuracy high. Table 9 shows the maximum radius errors with the Continuous Motion NCTF controller under the three conditions. The maximum tracking errors in the motions are also listed in the table. The reference peripheral velocities in all of the conditions are 3.14 μm/s. In Table 9, the tracking errors decrease as the motion frequency becomes lower.

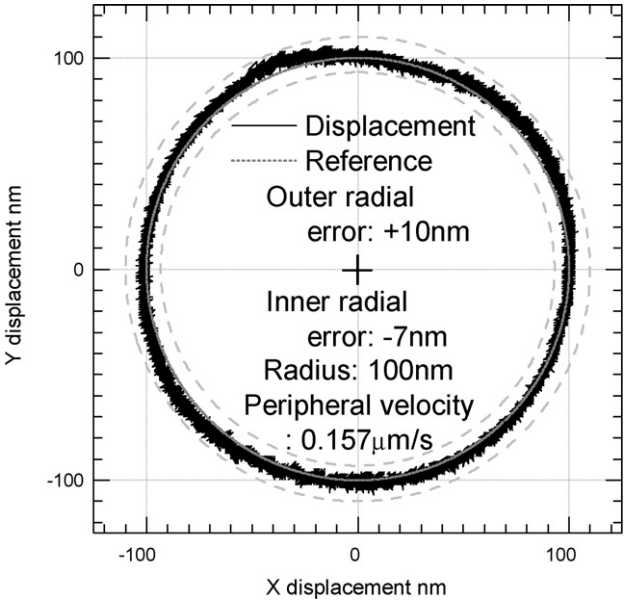

Fig. 17. Circular motion (radius: 100 nm, peripheral velocity: 0.157 μm/s, motion frequency: 0.25 Hz).

The difference between the errors of the Continuous Motion NCTF control system in Tables 2 and 5 is negligible, although their reference motion frequencies differ. Their reference peripheral velocities are equal to or higher than 15.7 mm/s. Velocities

Table 9
Motion control performances with the Continuous Motion NCTF controllers (1).

Frequency of the sinusoidal reference (radius of motion)	max $\lvert x_r - x \rvert$		max $\lvert y_r - y \rvert$		Maximum radial error	
	Average (nm)	Standard deviation (nm)	Average (nm)	Standard deviation (nm)	Average (nm)	Standard deviation (nm)
0.1 Hz (5 μm)	19.8	1.0	18.7	1.8	20.1	1.3
0.5 Hz (1 μm)	48.5	4.1	34.4	5.3	43.6	3.9
5 Hz (100 nm)	107.1	6.4	66.6	18.8	43.4	8.3

Table 10
Motion control performances with the Continuous Motion NCTF controllers (2).

Radius of circular motion (nm)	max $\lvert x_r - x \rvert$		max $\lvert y_r - y \rvert$		Maximum radial error	
	Average (nm)	Standard deviation (nm)	Average (nm)	Standard deviation (nm)	Average (nm)	Standard deviation (nm)
100	10.5	0.8	9.7	1.4	10.0	1.0

higher than those listed in Tables 2 and 5 are considered to cover over the influence of the frequency. Fig. 17 shows the experimental circular motion for which the reference peripheral velocity is 0.157 μm/s, which is much lower than that in Fig. 16. Table 10 lists the experimental errors obtained in the experiment. The maximum radius and the sinusoidal errors in Fig. 17 are approximately half those shown in Fig. 16.

5. Conclusions

In the present paper, the Continuous Motion NCTF controller was proposed as a high-performance and simple motion controller. The proposed controller was then applied to *X*- and *Y*-axis mechanisms for evaluation of its effectiveness. The Continuous Motion NCTF controller has almost the same structure as the conventional controller and is designed using the same design procedure. As a result, the controller structure is simple and the controller design is easy. A common Continuous Motion NCTF controller was implemented for the *X*- and *Y*-axis mechanisms. The motion control performances with the Continuous Motion NCTF controller were evaluated from experimental motion control results, including tracking, contouring, and positioning control results. The performances with the Continuous Motion NCTF controller were compared with those using the conventional NCTF and the PI-D controllers. The results prove that, overall, the performances obtained using the Continuous Motion NCTF controller is better than those obtained using the conventional NCTF and the PI-D controllers. They also indicate that the Continuous Motion NCTF controller is more suitable than the conventional NCTF controller in all the motion control including positioning. The Continuous Motion NCTF controller produced high precision motion, the accuracy of which was equal to or smaller than 10 nm.

Acknowledgement

This research was supported by a grant from the Electro-Mechanic Technology Advancing Foundation.

References

[1] Oiwa T, Katsuki M. Survey of questionnaire on ultra-precision positioning. J JSPE 2003;69(8):1077–82 [in Japanese].
[2] Ito A, Shiraishi M. Trend and some simple design examples of robust control in mechatronic systems. J JSPE 2000;66(5):811–5 [in Japanese].
[3] Wakui S. Current and future of precision positioning stage working in stepper. J JSPE 2001;67(2):202–6 [in Japanese].
[4] Maeda GJ, Sato K, Hashizume H, Shinshi T. Control of an XY nano-positioning table for a compact nano-machine tool. JSME Int J Ser C 2006;49(1):21–7.
[5] Tsuruta K, Murakami T, Futami S. Nonlinear friction behavior of discontinuity at stroke end in a ball guide way. J JSPE 2003;69(12):1759–63 [in Japanese].
[6] Suzuki Y, Matsubara A, Kakino Y, Tsutsui K. A stick motion compensation system with a dynamic model. JSME Int J Ser C 2004;47(1):168–74.
[7] Tan KK, Lim SY, Huang S, Dou HF, Giam TS. Coordinated motion control of moving gantry stages for precision applications based on an observer-augmented composite controller. IEEE Trans Control Syst Technol 2004;12(6):984–91.
[8] Sato K, Zheng J, Tanaka T, Shimokohbe A. Micro/macro dynamic characteristics of mechanism with a harmonic speed reducer and precision rotational positioning control using disturbance observer. JSME Int J Ser C 2000;43(2):318–25.
[9] Makino K, Sugimine M, Tomita Y. Development of precise XY-stage system for laser fine-cutting system. J JSPE 2001;67(1):65–9 [in Japanese].
[10] Iezawa M, Imagi A, Tomisawa M. High precision control of circular trajectory by disturbance cancellation. Proc MOVIC'98 1998;2:763–8.
[11] Ro PI, Shim W, Jeong S. Robust friction compensation for submicrometer positioning and tracking for a ball-screw-driven slide system. Prec Eng 2000;24:160–73.
[12] Chen CL, Jang MJ, Lin KC. Modeling and high-precision control of a ball-screwdriven stage. Prec Eng 2004;28:483–95.
[13] Han S. The position tracking control of precise servo systems with nonlinear dynamic friction using variable structure control and friction observer. JSME Int J Ser C 2002;45(3):784–93.
[14] Iwasaki M, Shibata T, Matsui N. Disturbance-observer-based nonlinear friction compensation in table drive system. IEEE/ASME Trans Mechatron 1999;4(1):3–8.
[15] Woronko A, Altintas Y. Piezoelectric tool actuator for precision machining on conventional CNC turning centers. Prec Eng 2003;27(4):335–45.
[16] Altintas Y, Erkorkmaz K, Zhu W-H. Sliding mode controller design for high speed feed drives. Ann CIRP 2000;49(1):265–70.
[17] Tan KK, Huang SN, Lee TH. Robust adaptive numerical compensation for friction and force ripple in permanent-magnet linear motors. IEEE Trans Magnetics 2002;38(1):221–8.
[18] Ramesh R, Mannan MA, Poo AN. Tracking and contour error control in CNC servo systems. Int J Mach Tools Manuf 2005;45:301–26.
[19] Butler J, Hacck B, Tomizuka M. Reference input generation for high speed coordinated motion of a two axis system. J Dyn Syst Meas Control 1991;113:67–74.
[20] Weck M, Ye G. Sharp corner tracking using the IKF control strategy. Ann CIRP 1990;39(1):437–41.
[21] Endo S, Kobayashi H, Kempf CJ, Kobayashi S, Tomizuka M, Hori Y. Robust digital tracking controller design for high-speed positioning systems. Control Eng Pract 1996;4(4):527–36.
[22] Tarng YS, Chuang HY, Hsu WT. An optimization approach to the contour error control of CNC machine tools using genetic algorithms. Int J Adv Manuf Technol 1997;13:359–66.
[23] Lee M-H, Yang S-H, Kim YS, Roh Y-R, Kim C. A multi-axis contour error controller for free form curves. JSME Int J Ser C 2004;47(1):144–9.
[24] Srinivasan K, Kulkarni PK. Cross-coupling control of biaxial feed drive servomechanisms. J Dyn Syst Meas Control 1990;112:225–32.
[25] Wahyudi, Sato K, Shimokohbe A. Characteristics of Practical control for point-to-point (PTP) positioning systems effect of design parameters and actuator saturation on positioning performance. Prec Eng 2003;27:157–69.
[26] Sato K, Nakamoto K, Shimokohbe A. Practical control of precision positioning mechanism with friction. Prec Eng 2004;28:426–34.
[27] Sato K, Maeda GJ, Wahyudi. Practical control of a ball screw mechanism for ultraprecision positioning. In: Proceedings of ICPT 2006. 2006. p. 217–8.
[28] Sato K, Wahyudi, Shimokohbe A. Practical control for two-mass positioning mechanism. In: Proceedings of the 1st Korea–Japan Conference on Positioning Technology. 2002. p. 206–11.
[29] Maeda GJ, Sato K. Practical control method for ultra-precision positioning using a ballscrew mechanism. Pec Eng 2008;32:309–18.
[30] Sato K, Maeda GJ. Practical ultraprecision positioning of a ball screw mechanism. Int J Precision Eng Manuf 2008;9(2):44–9.
[31] Ishikawa J, Hattori T, Hashimoto M. High-speed positioning control for hard disk drives based on two-degree-of-freedom control. Trans JSME Ser C 1996;62(597):1848–56 [in Japanese].
[32] Nakagawa S, Yamaguchi T, Numasato H, Hosokawa H, Hirai H. Improving the disturbance resistance of magnetic disk drives by using anti-windup and model following controls with initial value compensation. JSME Int J Ser C 2000;43(3):618–24.
[33] Ihara Y. Contouring accuracy performance of machine tools with recent conventional numerical controller. Proc LEM21 2005;2:465–8.